Original Research

Quantitative Myocardial Perfusion Analysis With a Dual-Bolus Contrast-Enhanced First-Pass MRI Technique in Humans

Li-Yueh Hsu, DSc, Kenneth L. Rhoads, MD, Jessica E. Holly, BSc, Peter Kellman, PhD, Anthony H. Aletras, PhD, and Andrew E. Arai, MD*

Purpose: To compare fully quantitative and semiquantitative analysis of rest and stress myocardial blood flow (MBF) and myocardial perfusion reserve (MPR) using a dual-bolus first-pass perfusion MRI method in humans.

Materials and Methods: Rest and dipyridamole stress perfusion imaging was performed on 10 healthy humans by administering gadolinium contrast using a dual-bolus protocol. Ventricular and myocardial time-signal intensity curves were generated from a series of T1-weighted images and adjusted for surface-coil intensity variations. Corrected signal intensity curves were then fitted using fully quantitative model constrained deconvolution (MCD) to quantify MBF (mL/min/g) and MPR. The results were compared with semiquantitative contrast enhancement ratio (CER) and upslope index (SLP) measurements.

Results: MBF (mL/min/g) estimated with MCD averaged 1.02 ± 0.22 at rest and 3.39 ± 0.59 for stress with no overlap in measures. MPR was 3.43 ± 0.71, 1.91 ± 0.65, and 1.16 ± 0.19 using MCD, SLP, and CER. Both semiquantitative parameters (SLP and CER) significantly underestimated MPR ($P < 0.001$) and failed to completely discriminate rest and stress perfusion.

Conclusion: Rest and stress MBF (mL/min/g) and MPR estimated by dual-bolus perfusion MRI fit within published ranges. Semiquantitative methods (SLP and CER) significantly underestimated MPR.

Key Words: magnetic resonance imaging; myocardial perfusion; myocardial blood flow; myocardial perfusion reserve; contrast agent; gadolinium
J. Magn. Reson. Imaging 2006;23:315–322.
Published by Wiley-Liss, Inc.

FIRST-PASS PERFUSION MRI uses a series of T1-weighted images during passage of a contrast bolus through the heart to characterize myocardial blood flow (MBF). MBF (expressed in mL/min/g) and myocardial perfusion reserve (MPR; defined as the ratio of hyperemic and resting blood flow) are both clinically important indices for assessing myocardial ischemia.

Single-bolus first-pass animal studies have shown that MBF and MPR can be reliably estimated from the time-signal intensity curves of first-pass MR perfusion images through numerical deconvolution (1,2). Analyses of the time-signal intensity curves derived from the single-bolus perfusion images showed good inter- and intraobserver agreement in patient studies (3), and demonstrated quantifiable MBF during rest and hyperemia perfusion in healthy human subjects (4). Due to nonlinearity between signal intensity and gadolinium concentration inherent to the MR acquisition, however, it is necessary to limit the dose of contrast in this type of first-pass study (5).

The dual-bolus first-pass perfusion MRI method was recently introduced to allow the use of high concentrations of contrast for myocardial analysis, but a lower concentration bolus to maintain the linearity of the left ventricle (LV) signal intensity (6). This method has been validated in an animal model against microsphere blood flow, and has shown good correlations across a range of low, normal, and hyperemic MBF (6). The results of these experimental studies suggest that commonly used semiquantitative methods based on the contrast enhancement ratio (CER) (7,8) or upslope index (SLP) (9–11) underestimate MPR compared to fully quantitative methods (1–6).

In this study we aimed to apply fully quantitative analysis of dual-bolus first-pass perfusion MR images in healthy humans to determine rest MBF, stress MBF, and MPR. The results of the fully quantitative analysis were compared with semiquantitative measures of CER and SLP for separate rest and stress perfusion studies.

MATERIALS AND METHODS

Rest and stress first-pass perfusion images were acquired from 10 healthy volunteers (defined as having

Laboratory of Cardiac Energetics, National Heart Lung and Blood Institute, National Institutes of Health, Department of Health and Human Services, Bethesda, Maryland, USA.

Contract grant sponsor: National Heart, Lung, and Blood Institute.

*Address reprint requests to: A.E.A., Laboratory of Cardiac Energetics, National Heart, Lung, and Blood Institute, National Institutes of Health, 10 Center Dr., MSC 1061, Building 10, Room B1D-416, Bethesda, MD 20892-1061. E-mail: araia@nih.gov

Received March 25, 2005; Accepted November 17, 2005.
DOI 10.1002/jmri.20502
Published online 6 February 2006 in Wiley InterScience (www.interscience.wiley.com).

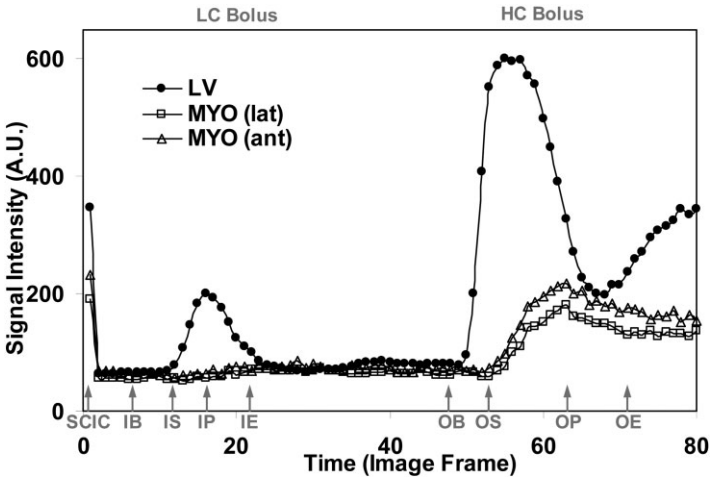

Figure 1. Time-signal intensity curves for dual-bolus first-pass perfusion MR image analysis. Raw time-signal intensity curves of the LV cavity (●) and two myocardial sectors (□: lateral, Δ: anterior) from a stress perfusion study are illustrated. Two imaging stages are cascaded to produce a continuous time-signal intensity plot: contrast enhancement images after low-concentration (LC bolus) contrast administration, followed by high-concentration (HC bolus) contrast administration. In addition, a reference image acquired at the beginning of the imaging before contrast delivery is used for SCIC. The time frames of interest, as indicated in the continuous time-signal intensity plot: input baseline frame (IB), input start frame (IS), input peak frame (IP), input end frame (IE), output baseline frame (OB), output start frame (OS), output peak frame (OP), and output end frame (OE).

a 10-year risk of coronary artery disease of <2% based on the Framingham risk factor analysis). All studies were performed following protocols approved by the Institutional Review Board of the National Institutes of Health.

Image Acquisition

Rest and stress perfusion imaging was performed with a dual-bolus protocol using 0.005 mmol/kg and 0.1 mmol/kg of gadolinium-DTPA (Magnevist; Berlex Laboratories, Wayne, NJ, USA) diluted to provide injections of equal volumes and flushed with saline at 5 mL/sec flow rate (Medrad, Indianola, PA, USA) as previously described (6). At least two hours after rest perfusion, 0.56 mg/kg of intravenous dipyridamole was infused over four minutes for the stress study. To minimize the breath-hold time, the low-concentration bolus was administered during a first breath-hold, and the high-concentration bolus was given during a second breath-hold after the subject was allowed to take two to four large breaths between the two scans. A series of T1-weighted images were acquired by using a saturation prepared segmented gradient echo-planar sequence on a 1.5T scanner (GE Medical Systems, Waukesha, WI, USA). Three slice locations (basal, mid, and apical) were acquired every R-R interval for a period lasting 40–50 heartbeats. Typical imaging parameters included a saturation preparation pulse at flip angle = 70–90°, saturation recovery time = 60 msec, repetition time (TR) = 6.6 msec, echo time (TE) = 1.6 msec, echo train length = 4, bandwidth = ±125 kHz, acquisition matrix = 128 × 72, field of view (FOV) = 360 × 270 mm, flip angle = 20°, slice thickness = 8 mm, and temporal resolution = 120 msec.

Image Analysis

Each perfusion slice was divided into either six sectors (at the basal and mid locations) or four sectors (at the apex) according to the 16-segment model of the American Society of Echocardiography. Time-signal intensity curves of myocardial regions of interest (ROIs) were generated and analyzed using custom software written in Interactive Data Language (Research Systems Inc., Boulder, CO, USA). Contours of the LV epicardial and endocardial borders were manually traced on each image. The myocardium was then subdivided into radial sectors of equal size. Time-signal intensity curves of the LV cavity and the myocardial sectors were generated for both low- and high-concentration contrast boluses.

In first-pass perfusion imaging, the time-signal intensity measurements within the heart reflect the contrast concentration during the wash-in and wash-out of the bolus. Figure 1 shows typical time-signal intensity curves of a dual-bolus first-pass perfusion MR study. Before the contrast boluses were delivered, a proton-density-weighted reference image was acquired at the beginning of imaging, using a small magnetization flip angle (5°) and no saturation preparation pulse for surface coil intensity correction (SCIC).

In the time-signal intensity plot (Fig. 1), several time frames of interest from the low-concentration bolus (input) and high-concentration bolus (output) curves are indicated: input baseline frame (IB), input start frame (IS), input peak frame (IP), input end frame (IE), output baseline frame (OB), output start frame (OS), output peak frame (OP), and output end frame (OE). These time frames of interest were selected by the user to provide the analysis software with initial timing values for important features relevant to the quantitative and semi-quantitative measurements. Baseline frames (IB and OB) were used to adjust the value of the input and output signal intensity curves. Contrast starting frames (IS and OS) were selected as an initial position in time for the input and output curve alignment. Peak contrast frames (IP and OP) designated the maximum value of the LV and myocardial contrast enhancement over time. First-pass contrast ending frames (IE and OE) specified the time points before contrast recirculation arrived at the LV and myocardial ROIs.

The first step in our analysis of time-signal intensity curves was to correct the intensity variation due to the receiving surface coil sensitivity profile (B1 inhomogeneity). In our studies, signal intensity curves of the myocardial ROIs were normalized using the signal intensity value of the reference frame (SCIC), and the precontrast baseline signal intensity was subtracted

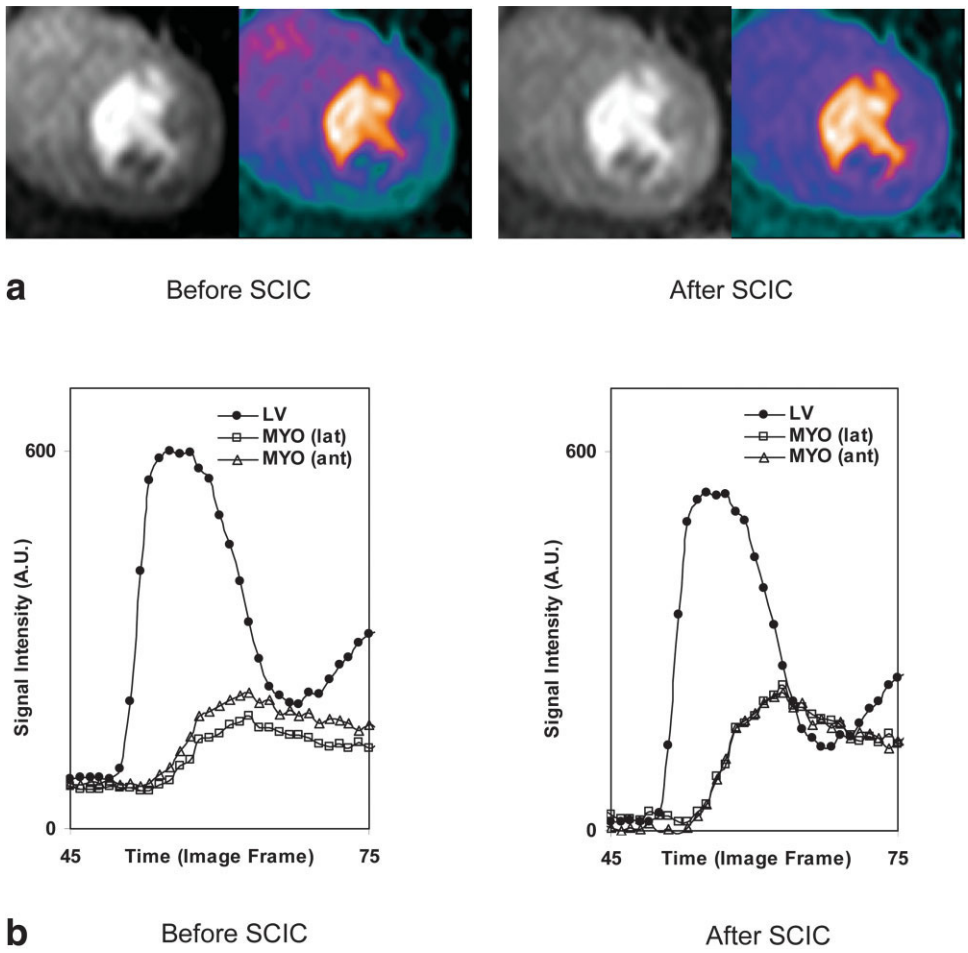

Figure 2. a: Following SCIC, the contrast-enhanced image shows more uniformly distributed myocardial intensities compared to the same image before the correction. **b:** Time-signal intensity curves of lateral and anterior sectors show a similar time-signal kinetic after the SCIC and baseline intensity adjustment.

from the signal intensity curves (IB and OB; Figs. 1 and 2). The LV signal intensity curve of the low-concentration bolus provides the input function, and the myocardial signal intensity curve after the high-concentration bolus describes the myocardial output function. Note that portions of the signal intensity curves that are used for analysis remain within the intrinsic dynamic range of the acquisition (Fig. 3). Figure 4 shows how perfusion measurements were performed on the time-signal intensity curves in our analysis. Three different techniques were compared: semiquantitative CER, semiquantitative SLP, and fully quantitative model constrained deconvolution (MCD). The MPR (as obtained by MCD) or MPR index (as obtained by SLP and CER) were computed for all three methods as a ratio of stress MBF (as obtained by MCD) or stress MBF index (as obtained by SLP and CER) divided by the corresponding rest measurements.

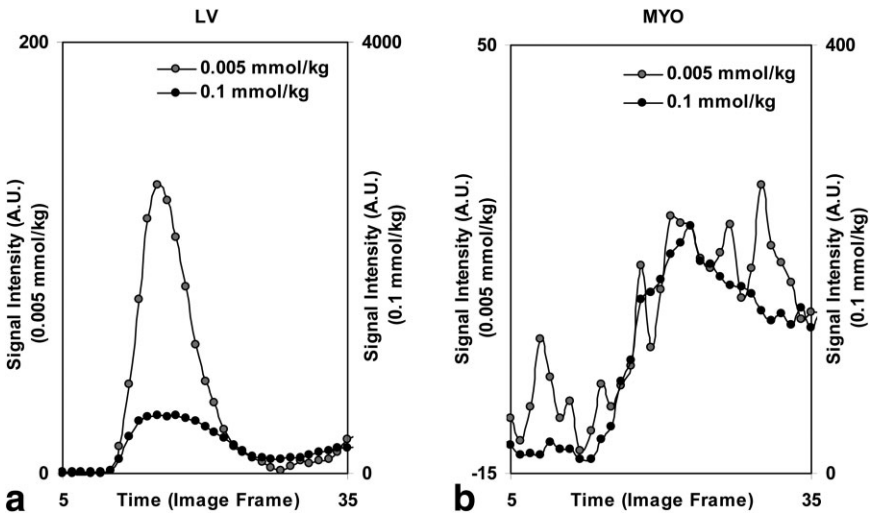

Figure 3. Comparison of time-signal intensity curves of the low-concentration (0.005 mmol/kg) and high-concentration (0.1 mmol/kg) contrasts during dual-bolus first-pass perfusion imaging. **a:** Nonlinearity of the MR signal is clearly observed in the LV intensity curve for the high-concentration bolus vs. the low-concentration bolus. **b:** The myocardial signal intensity curve after the low-concentration bolus, on the other hand, shows more beat-to-beat signal variation compared to the high-concentration bolus curve. The dual-bolus analysis uses the LV cavity signal from the low-concentration bolus, and the myocardial curve after the high-concentration bolus.

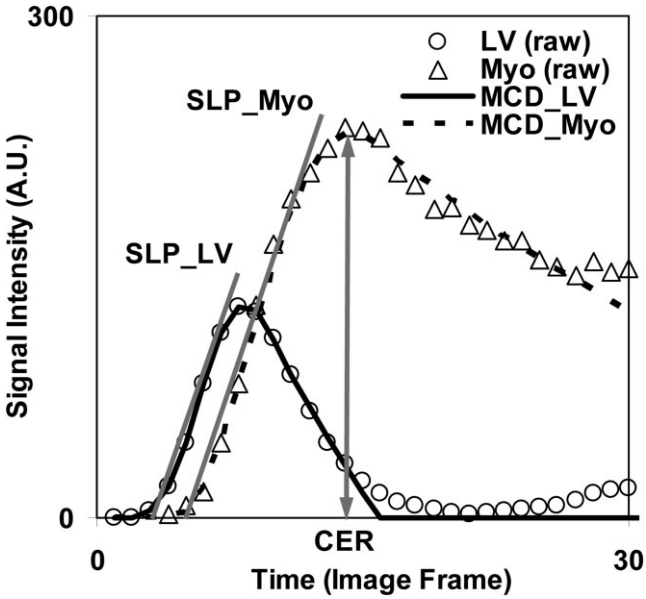

Figure 4. MPR is calculated using three different techniques: semiquantitative CER, semiquantitative SLP, and fully quantitative MCD. The fitted signal intensity curves of the blood cavity (MCD_LV) and myocardium (MCD_Myo) are used to calculate the MBF in the MCD method. The tail of the LV and Myo intensity curves are linearly extrapolated using the downslope after the peak intensity to avoid the recirculation component. SLP is calculated using the myocardial upslope (SLP_Myo) and is normalized by the LV upslope (SLP_LV) measurements. CER is measured at the peak enhancement of the myocardial intensity curve and divided by the baseline value.

CER Method

The CER was calculated as follows:

$$\mathrm{CER} = \frac{(SI_{peak} - SI_{baseline})}{SI_{baseline}}.$$

where SI_{peak} is the peak signal intensity of a myocardial ROI, and $SI_{baseline}$ is the baseline signal intensity of the same region. The CER is a measure of peak myocardial contrast enhancement after baseline signal intensity adjustment. This measurement reflects the maximum enhancement in the myocardium and ignores the temporal characteristics, such as the rate of the contrast enhancement.

SLP Method

The SLP was calculated as the slope of myocardial signal intensity curves divided by the slope of the LV curve measured from consecutive acquisition frames (more than three for the LV, and more than five for the myocardium, on average). It is a measurement of the early phase of signal intensity increase during the contrast wash-in that ignores the portion in which the slope begins to decrease. This measurement considers the maximum rate of contrast delivery into the myocardium. The ratio of the myocardial-to-LV upslope (SLP_Myo divided by SLP_LV; Fig. 4) was calculated as a perfusion index for each myocardial ROI. This method considers some extent of LV input variations by using a normalization factor calculated from the LV input function.

MCD Method

The MCD was based on the central volume principle introduced by Zierler (12,13), which describes the theoretical foundations of the indicator-dilution method for measuring blood flow and blood volume. In an imaging indicator-dilution experiment, a bolus of contrast material is injected into an upstream input site, where a time sequence of images is acquired as the contrast flows through a measuring organ or tissue output site (14,15).

Assuming a constant tissue flow rate, F, the quantity of contrast present in the tissue region at any time, $q(t)$, can be calculated from the difference between the input and output contrast concentration curves $C_{in}(t)$ and $C_{out}(t)$,

$$q(t) = F\int_0^t [C_{in}(s) - C_{out}(s)]ds$$

.

Assuming the transport within a tissue region to be linear and stationary, the response of the region to an arbitrary input can be obtained by the convolution of such input with a tissue impulse response,

$$C_{out}(t) = \int_0^t C_{in}(t-\tau)h(\tau)d\tau = C_{in}(t) \times h(t).$$

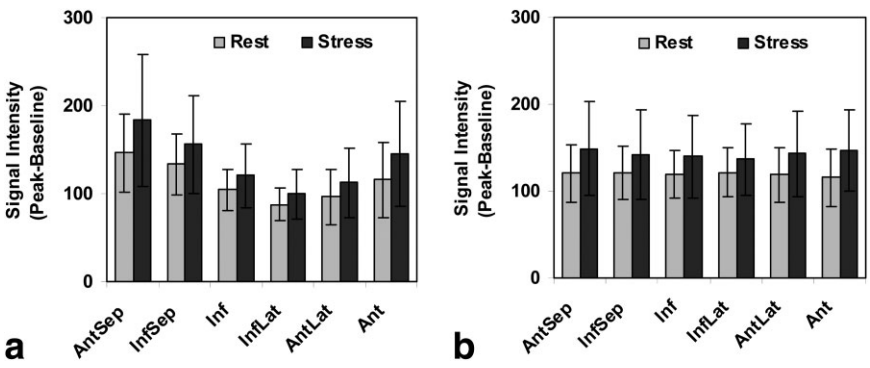

Figure 5. Regional signal intensity measurements (mean ± SD) of the contrast enhancement (peak minus baseline intensities) before (**a**) and after (**b**) SCIC and baseline intensity adjustment. Note that the signal variation across different segments is reduced after SCIC (b).

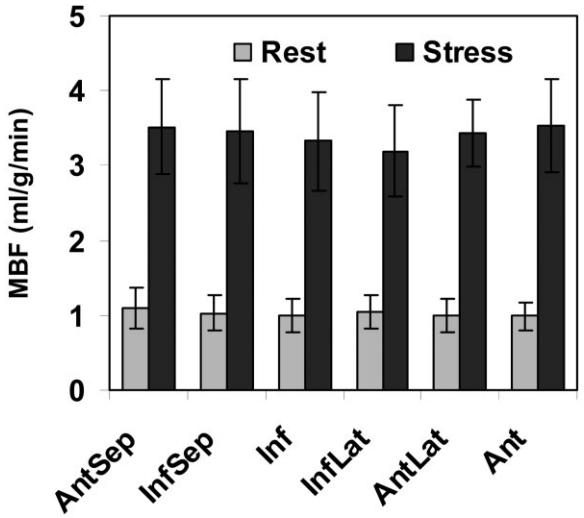

Figure 6. Regional MBF measurements (mean ± SD) from the rest and stress perfusion studies using fully quantitative MCD.

This tissue impulse response function, $h(t)$, represents an amplitude-scaled probability density function of contrast transits through the tissue region. When the input of the contrast is a Dirac delta function $C_{in}(t) = \delta(t)$, and under the conditions that $C_{in}(t < 0) = 0$ and $C_{out}(t = 0) = 0$, the initial amplitude of the tissue impulse response function can be derived as $h(t = 0) = F$.

A Fermi function was previously used as a model to approximate the tissue impulse response of the myocardial transfer function during contrast transit (1,16). The shape of the Fermi function was observed to be similar to the impulse response of an intravascular contrast agent. However, a Fermi function model-based analysis must be restricted within the first pass of an extracellular contrast, such as GD-DTPA, when the signal intensity curve responds more to the change of flow and less to the interstitial contrast exchange. The impulse response *h(t)* describes a general relationship between the arterial input *LV(t)* and myocardial output *Myo(t)* functions in a linear time-invariant system as a time convolution process *Myo(t) = LV(t) * h(t).* It characterizes the frequency of the contrast transit from the LV cavity into the myocardium. As outlined by Zierler (12,13), the initial amplitude of the impulse response of a tissue region equals the MBF through that region in response to an instantaneous input (a direct delta function) of contrast arrival. The Fermi function has three parameters to be optimized:

$$h(t) = \frac{F}{1 + \exp[-(t - \tau) \cdot k]},$$

where F represents the magnitude of the function, and τ and k describe the temporal delay length and decay rate of *h(t)* due to contrast wash-out. In a dual-bolus acquisition, the LV input curve was acquired several heartbeats before the myocardial output intensity curves. Thus, a time delay (t_d) was added to the input function as an additional parameter for numerical optimization: $Myo(t) = LV(t\text{-}t_d) * h(t)$. The initial estimate of this time delay was calculated from the user-selected contrast starting frames (IS and OS) and then optimized during the curve fitting. A freely available implementation (17) of the Marquardt-Levenberg iterative algorithm (18,19) was used for the nonlinear least-squares curve fitting in this study.

As shown in Fig. 4, the tail of the LV input and myocardial output intensity curves were linearly extrapolated using the downslope calculated between time points of the peak intensity (IP and OP) and the first-pass contrast ending (IE and OE) frames. As suggested in Refs. 20 and 21, this extrapolated downslope can be used to extend the linear portion of the signal intensity curve during indicator dilution (contrast wash-out) and represents the expected values in the absence of recirculation. These extended intensity curves also add the benefit that the output fitting curve is attached to the early phase of the myocardial downslope and thus the numerical deconvolution of the MCD method is stabilized.

RESULTS

All subjects (two men and eight women, mean age = 33 ± 4 years) tolerated the scans without adverse events. The average heart rate was 64 ± 10 for the rest perfusion study and increased to 89 ± 13 during dipyridamole stress ($P < 0.001$). The systolic blood pressure averaged 114 ± 8 at rest and decreased to 106 ± 12 ($P = 0.05$) during stress. The diastolic blood pressure did not change significantly (68 ± 7 vs. 64 ± 12, $P = 0.34$).

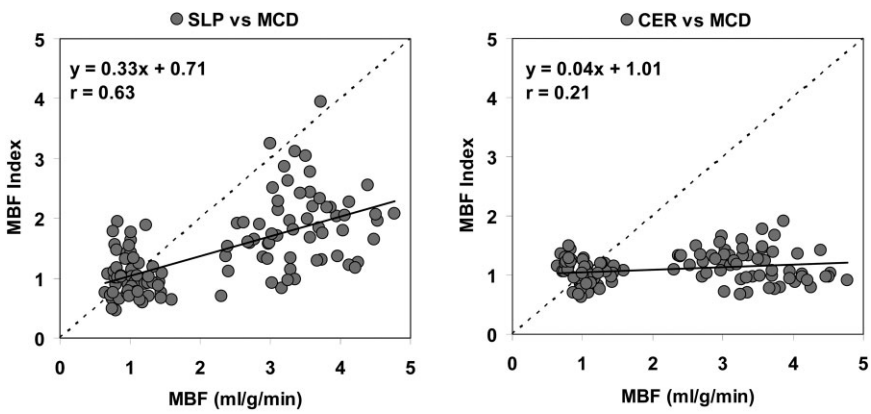

Figure 7. Scatter correlation plot illustrates the relationship between MBF measured by fully quantitative MCD vs. MBF index measured by semiquantitative CER and semiquantitative SLP. MBF indices of CER and SLP were linearly normalized to MCD rest MBF for both rest and stress measurements. The use of semiquantitative SLP and CER measures led to substantially underestimated vasodilated MBF values.

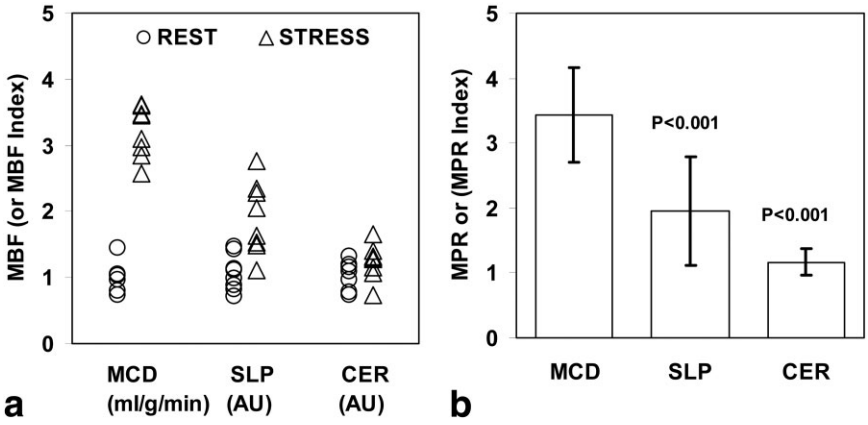

Figure 8. (**a**) MBF and (**b**) MPR from 10 normal volunteers compared using three different techniques: semiquantitative CER, semiquantitative SLP, and fully quantitative MCD. The MBF indices of CER and SLP were linearly normalized to MCD rest MBF for both rest and stress measurements. Both CER and SLP semiquantitative analysis underestimated MPR compared to the fully quantitative MCD method ($P < 0.001$).

An example of time-signal intensity curves from one stress perfusion study is shown in Fig. 1. The maximum LV cavity signal amplitude was markedly attenuated during the high-concentration bolus (0.1 mmol/kg) compared to the expected signal intensity of the scale-adjusted (×20) low-concentration bolus (0.005 mmol/kg). A brief analysis of the relationship between contrast concentrations and signal intensity is provided in the Appendix. The degree of underestimation of the LV signal during the high-concentration bolus can be appreciated when it is scaled and superimposed with the LV curve during the low-concentration bolus (Fig. 3a). For our data overall, the peak amplitude of the LV signal intensity was only 3.41 ± 0.70-fold higher for the high-concentration bolus compared to the low-concentration bolus. Most importantly, this attenuation was not linear and resulted in a distorted LV input function after the high-concentration bolus. In contrast, the quality of the signal intensity curve derived from a myocardial ROI during the low-concentration bolus is much more variable compared to the same region during the high-concentration bolus when the two are scaled comparably (Fig. 3b). Thus, all analyses in our study used the signal intensity curve of the LV during the low-concentration bolus to define the input function, and the signal intensity curves after the high-concentration bolus to define the myocardial output measurements for blood flow estimation (Fig. 4).

Figure 2 shows the effects of SCIC. The color-coded image prior to SCIC shows more distinct color shading on the myocardium, with the anterior septum region being brighter than the inferior and lateral walls. After SCIC the signal intensity is much more uniform around the short axis of the heart. The effects on signal intensity curves for anterior vs. lateral regions also demonstrate that two regions with visually different upslopes prior to SCIC become virtually superimposed after SCIC and baseline intensity adjustment.

For the group data overall, Fig. 5 shows the results of regional signal intensity variation during the contrast enhancement (peak minus baseline intensities) before and after the SCIC and baseline intensity adjustment. The coefficient of variation was significantly reduced from 0.23 to 0.06 for rest perfusion, and from 0.23 to 0.08 for stress perfusion after these intensity adjustments were made ($P < 0.001$).

The regional MBF estimated with the fully quantitative MCD is shown in Fig. 6. The relationship between MBF measured by fully quantitative MCD (MCD) vs. MBF index measured by semiquantitative CER and semiquantitative SLP is shown in Fig. 7. For the group data overall, MBF averaged 1.02 ± 0.22 mL/min/g at rest and 3.39 ± 0.59 mL/min/g during stress (Fig. 8a). There was no overlap between the rest and stress estimates of MBF with the MCD method. However, using exactly the same signal intensity curves, both semiquantitative CER and SLP measures failed to completely distinguish stress from rest perfusion (Fig. 8a). The amount of overlap was more severe for CER than SLP, and no threshold completely discriminated rest from stress perfusion studies.

The MPR was 3.43 ± 0.71 using the MCD (Fig. 8b). MPR indices were 1.91 ± 0.65, and 1.16±0.19 for the SLP and CER measurements, respectively (Fig. 8b). Both semiquantitative SLP and CER methods underestimated MPR compared to the fully quantitative MCD technique ($P < 0.001$).

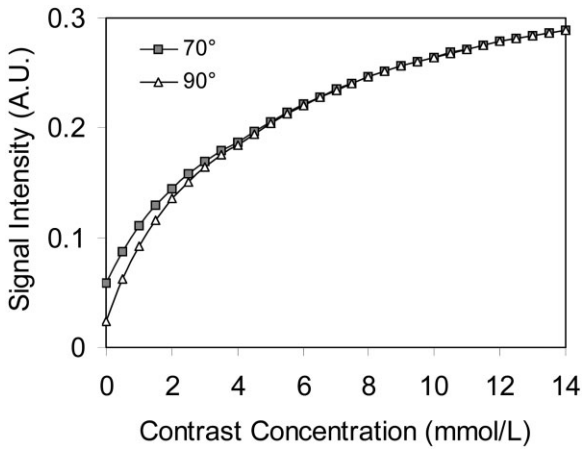

Figure 9. Relaxivity curves plotting signal intensity values vs. contrast concentration for the image acquisition parameters used in this study. For low contrast concentrations, a 70° flip angle gives a higher SNR and is slightly more linear in the range of 0–2 mmol/L. However, a 90° flip angle provides a higher CNR of blood and myocardium within the same range.

DISCUSSION

With the dual-bolus contrast approach, the time-signal intensity characteristics of the LV input function are well represented by the low-concentration bolus, since it remains safely within the linear range of the imaging experiment (see Appendix). High-quality myocardial time-signal intensity curves are produced after the high-concentration bolus. As a result, images after the high-concentration bolus administration maintain a high signal-to-noise ratio (SNR) that is suitable for both qualitative visual interpretation and fully quantitative analysis. When this dual-bolus MRI technique was applied to normal volunteer studies, MPR obtained by fully quantitative MCD differentiated stress and rest MBF to a greater extent than semiquantitative methods based on CER or SLP. The underestimation of perfusion reserve by the semiquantitative measures erroneously compresses the effects of vasodilation into a narrower range of values, which may explain why clinical techniques using SLPs to estimate perfusion reserve choose a low threshold (between 1.1 and 1.5) to discriminate ischemic from normal regions (9–11).

The current study in humans confirms many of the observations made in a previous canine model using the dual-bolus perfusion imaging technique (6). The quality of the raw signal intensity curves measured in humans is quite comparable to that seen in the animal studies. The SLP and CER measurements in humans revealed degrees of relative underestimation of vasodilated blood flow similar to those observed in animals. As predicted (but not reported) in the canine study, the semiquantitative measures underestimated MPR.

In a dual-bolus study, the peak signal amplitude of the myocardium during the high-concentration bolus is similar to the peak signal amplitude of the LV cavity during the low-concentration bolus (Fig. 1). However, the myocardial signal intensity is modulated by multiple factors: high gadolinium concentration in the vascular space, a gradually increasing concentration in the interstitial space, and the extent to which gadolinium in either of these compartments affects intracellular protons as a result of water exchange between these compartments. Thus, one should use caution when interpreting the myocardial signal intensity.

It is important to account for the receiving surface coil intensity profile, since the raw signal intensity of the myocardial regions is systematically affected in a spatially varying manner. In our studies this signal intensity variation is calibrated using a proton-density-weighted reference image acquired prior to contrast administration. We have found that this produces a much more reliable SCIC than using a heavily T1-weighted image prior to contrast arrival in the myocardium.

In summary, in this study we performed dual-bolus first-pass perfusion MRI on healthy normal volunteers. The MPR averaged 3.43, using quantitative MCD, which fits within published ranges (1). Semiquantitative methods (SLP and CER) significantly underestimated MPR and effectively diminished the benefit of increased blood flow during vasodilation. Since the semiquantitative perfusion reserve indices underestimate vasodilated flow it becomes necessary to use low cutoff values (9–11) to differentiate ischemic from normal perfusion—a problem that could be improved by fully quantitative analysis.

APPENDIX

The relationship of contrast concentration vs. signal intensity values was simulated using the method described by Sekihara (22). Theoretical T1 curves of both 70° and 90° saturation pulses were calculated using the imaging parameters described in the Materials and Methods section. The T1 values in the curve were then converted to the contrast concentration values using the equation $\frac{1}{T_1} = \frac{1}{T_{1\,blood}} + \gamma[Gd]$, where $T_{1\,blood}$ is the T_1 value of the blood without contrast, $[Gd]$ is the concentration of the contrast, and γ is the relaxivity of the Gd. For a 70-kg person, the maximum LV contrast concentration was estimated at 14 mmol/L for the high-concentration bolus, and 0.7 mmol/L for the low-concentration bolus (5). As plotted in Fig. 9, although the low-concentration bolus stays in the linear range, the high-concentration bolus does not, and the LV cavity signal intensity increases only three- to fourfold despite a 20-fold higher dose.

REFERENCES

1. Jerosch-Herold M, Wilke N, Stillman AE, Wilson RF. MR quantification of the myocardial perfusion reserve with a Fermi function model for constrained deconvolution. Med Phys 1998:25:73–84.
2. Jerosch-Herold M, Swingen C, Seethamraju RT. Myocardial blood flow quantification with MRI by model-independent deconvolution. Med Phys 2002:29:886–897.
3. Muhling OM, Dickson ME, Zenovich A, et al. Quantitative magnetic resonance first-pass perfusion analysis: inter- and intraobserver agreement. J Cardiovasc Magn Reson 2001:3:247–256.
4. Muehling OM, Jerosch-Herold M, Panse P, et al. Regional heterogeneity of myocardial perfusion in healthy human myocardium: assessment with magnetic resonance perfusion imaging. J Cardiovasc Magn Reson 2004:6:499–507.
5. Epstein FH, London JF, Peters DC, et al. Multislice first-pass cardiac perfusion MRI: validation in a model of myocardial infarction. Magn Reson Med 2002:47:482–491.
6. Christian TF, Rettmann DW, Aletras AH, et al. Absolute myocardial perfusion by MRI using a dual-bolus first-pass method: benefits over qualitative and semi-quantitative analysis. Radiology 2004: 232:677–684.
7. Wilke N, Simm C, Zhang J, et al. Contrast-enhanced first pass myocardial perfusion imaging: correlation between myocardial blood flow in dogs at rest and during hyperemia. Magn Reson Med 1993:29:485–497.
8. Kraitchman DL, Wilke N, Hexeberg E, et al. Myocardial perfusion and function in dogs with moderate coronary stenosis. Magn Reson Med 1996:35:771–780.
9. Al-Saadi N, Nagel E, Gross M, et al. Noninvasive detection of myocardial ischemia from perfusion reserve based on cardiovascular magnetic resonance. Circulation 2000:101:1379–1383.
10. Al-Saadi N, Nagel E, Gross M, et al. Improvement of myocardial perfusion reserve early after coronary intervention: assessment with cardiac magnetic resonance imaging. J Am Coll Cardiol 2000: 36:1557–1564.
11. Nagel E, Klein C, Paetsch I, et al. Magnetic resonance perfusion measurements for the noninvasive detection of coronary artery disease. Circulation 2003:108:432–437.

12. Zierler KL. Theoretical basis of indicator-dilution methods for measuring flow and volume. Circ Res 1962:10:393–407.
13. Zierler KL. Equations for measuring blood flow by external monitoring of radioisotopes. Circ Res 1965:16:309–321.
14. Clough V, Al-Tinawi A, Linehan JH, Dawson C. Regional transit time estimation from image residue curves. Ann Biomed Eng 1994: 22:128–143.
15. Jerosch-Herold M, Seethamraju RT, Swingen CM, Wilke NM, Stillman AE. Analysis of myocardial perfusion MRI. J Magn Reson Imaging 2004:19:758–770.
16. Axel L. Tissue mean transit time from dynamic computed tomography by a simple deconvolution technique. Invest Radiol 1983:18:94–99.
17. http://cow.physics.wisc.edu/~craigm/idl/fitting.html
18. Levenberg K. A method for the solution of certain problems in least squares. Q Appl Math 1944:2:164–168.
19. Marquardt D. An algorithm for least-squares estimation of nonlinear parameters. SIAM J Appl Math 1963:11:431–441.
20. Hamilton WF, Remington JW. Comparison of the time concentration curves in arterial blood of diffusible and non-diffusible substances when injected at a constant rate and when injected instantaneously. Am J Physiol 1947:148:35–39.
21. Meier P, Zierler KL. On the theory of indicator-dilution method for measurement of blood flow and volume. J Appl Physiol 1954:6:731–744.
22. Sekihara K. Steady-state magnetizations in rapid NMR imaging using small flip angles and short repetition intervals. IEEE Trans Med Imaging 1987:6:157–164.